Formation and Autoionization of a Dipole-Forbidden Superexcited State of CS_2

Yasumasa Hikosaka [†,§] **and Koichiro Mitsuke*** [*,†,‡]

Department of Vacuum UV Photoscience, Institute for Molecular Science, Myodaiji, Okazaki 444-8585, Japan, and Department of Structural Molecular Science, The Graduate University for Advanced Studies, Myodaiji, Okazaki 444-8585, Japan

Received: March 26, 2001; In Final Form: June 14, 2001

Two-dimensional photoelectron spectroscopy has been performed in the photon energy region of 14.60−15.35 eV, to investigate forbidden superexcited states of CS_2. The two-dimensional photoelectron spectra for the $CS_2^+(\tilde{X}\ ^2\Pi_g)$ and $CS_2^+(\tilde{B}\ ^2\Sigma_u^+)$ bands show remarkable formation of vibrational levels excited with one quantum of the antisymmetric vibrational mode at $E_{h\nu} \sim 14.88$ eV. The vibrational excitation is attributable to autoionization from a dipole-forbidden superexcited state which is formed through vibronic interaction with the $5p\sigma_u$ Rydberg state converging to $CS_2^+(\tilde{C}\ ^2\Sigma_g^+)$. The forbidden superexcited state is assigned as the $v = 1$ vibrational state in the ν_3 mode of the $3d\sigma_g$ Rydberg member converging to $CS_2^+(\tilde{C}\ ^2\Sigma_g^+)$. Preference in the autoionization of the forbidden superexcited state is discussed.

Introduction

Electronic transition into an excited state whose symmetry differs from that of any component of the electric dipole moment vector is forbidden from the totally symmetric ground state on the basis of the electric dipole transition and Born−Oppenheimer approximations. Nevertheless, forbidden electronic transitions occasionally take place. One of their origins is the vibronic interaction, where a forbidden state is mixed with an allowed state through asymmetric vibrational motion. The intensity borrowing from the allowed transition generates the strength of the forbidden transitions. In such cases, the proximity between the potential energies of the involved states is an important factor for an effective intensity borrowing. It generally happens that, on account of high state densities in the vacuum ultraviolet region, electronic transitions to forbidden superexcited states are endowed with enough strengths by the vibronic interaction. We have, however, much difficulty in recognizing and properly assigning such forbidden transitions by the use of conventional spectroscopic methods, since the obtained spectral features are already complicated by plenty of intense allowed transitions.

When the vibronic interaction exerts influence on the electronic transition from the ground $\tilde{X}\ ^1\Sigma_g^+$ state of a $D_{\infty h}$ triatomic molecule, population of vibronic species with symmetry of Σ_u^+ or Π_u becomes allowed. In other words, the direct product of symmetries of the electronic and vibrational parts must be Σ_u^+ or Π_u so that a vibronic state may be allowed in the electronic transition. Since the symmetries for the symmetric stretching ν_1, bending ν_2, and antisymmetric stretching ν_3 modes of the $D_{\infty h}$ triatomic molecules are ${\sigma_g}^+$, π_u, and ${\sigma_u}^+$, respectively, a vibrational level (v_1,v_2,v_3) of a forbidden state with a symmetry of Λ can be allowed when the direct product $\Lambda \times ({\sigma_g}^+)^{v_1} \times (\pi_u)^{v_2} \times ({\sigma_u}^+)^{v_3} = \Lambda \times (\pi_u)^{v_2} \times ({\sigma_u}^+)^{v_3}$ gives Σ_u^+ or Π_u. Here, we use the notation (v_1,v_2,v_3) to specify the vibrational level in which v_1, v_2, and v_3 quanta of the ν_1, ν_2, and ν_3 modes, respectively, are simultaneously excited. The above consideration on the direct product implies that forbidden superexcited states observed are accompanied by excitation of asymmetric vibration when the vibronic interaction works. One can then deduce that such forbidden superexcited molecules will autoionize into vibrationally excited ions in the asymmetric mode to a greater extent than ordinary allowed superexcited states.

Two-dimensional photoelectron spectroscopy provides photoelectron yields measured as a function of both incident photon energy and ionization energy. This spectroscopy enables us to study autoionizing feature of individual superexcited states, proving its powerfulness in assignments of allowed superexcited states and studies on the autoionization properties.[1−5] If forbidden superexcited states tend to have the above characteristic autoionizing features, we may discriminate them from other allowed states by making use of the two-dimensional photoelectron spectroscopy.

In the present work, we perform photoelectron spectroscopy of CS_2 to study its forbidden superexcited states in the photon energy region of 14.60−15.35 eV. The neutral ground state $\tilde{X}\ ^1\Sigma_g^+$ is of $D_{\infty h}$ symmetry with a valence shell electron configuration of $(5\sigma_g)^2(4\sigma_u)^2(6\sigma_g)^2(5\sigma_u)^2(2\pi_u)^4(2\pi_g)^4$. So far, spectra of CS_2 in the vacuum ultraviolet region have been measured with various experimental methods,[6−19] and most of the rich structures due to superexcited states have been assigned to dipole-allowed superexcited states. There also exists literature on a few dipole-forbidden superexcited states formed as a result of electronic quadrupole transitions.[19] However, forbidden states affected by vibronic interaction have not yet been recognized by these methods.

Experimental Section

The details of the experimental setup and procedure for photoelectron spectroscopy are described elsewhere[2−4] and will be presented here briefly. Measurements were performed at the beam line BL3B of the UVSOR Synchrotron Radiation Facility in Okazaki. The synchrotron radiation is dispersed using a 3 m

* Author to whom correspondence should be addressed. E-mail: Mitsuke@ims.ac.jp.
† Institute for Molecular Science.
‡ The Graduate University for Advanced Studies.
§ JSPS Research Fellow. Present address: Photon Factory, Institute of Materials Structure Science, Oho, Tsukuba 305-0801, Japan.

10.1021/jp011112v CCC: $20.00
Published on Web 08/10/2001

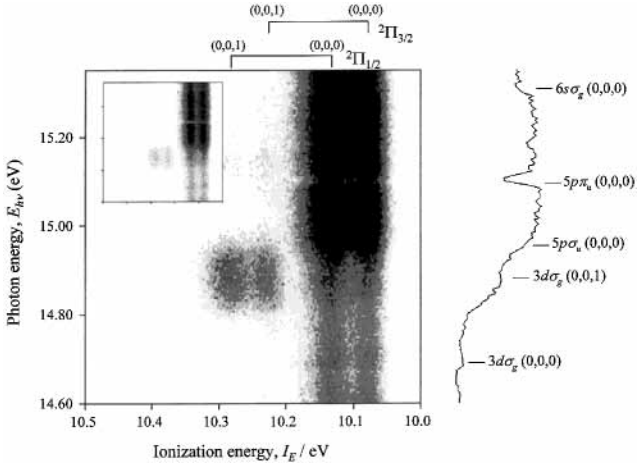

Figure 1. Two-dimensional photoelectron spectrum for the $CS_2^+(\tilde{X}\ ^2\Pi_g)$ band and its vicinities measured in the photon energy range of 14.60−15.35 eV. The electron yield is presented as a function of both photon energy $E_{h\nu}$ and ionization energy I_E by the plots with eight tones from light to dark on a linear scale. The curve in the right panel shows a constant ionic state spectrum, which is obtained by summing electron counts along the I_E axis at each $E_{h\nu}$. Five resonances of Rydberg states converging to $CS_2^+(\tilde{C}\ ^2\Sigma_g^+)$ are observed at $E_{h\nu}$ = 14.69, 14.88, 14.95, 15.09, and 15.31 eV. The former two states are first assigned in this work. The assignments for the latter three states are taken from refs 19 and 23.

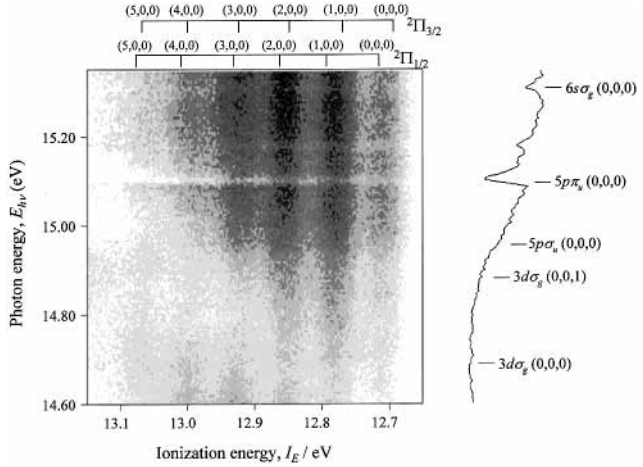

Figure 2. Two-dimensional photoelectron spectrum for the $CS_2^+(\tilde{A}\ ^2\Pi_u)$ band and its vicinities measured in the photon energy range of 14.60−15.35 eV. See the caption of Figure 1.

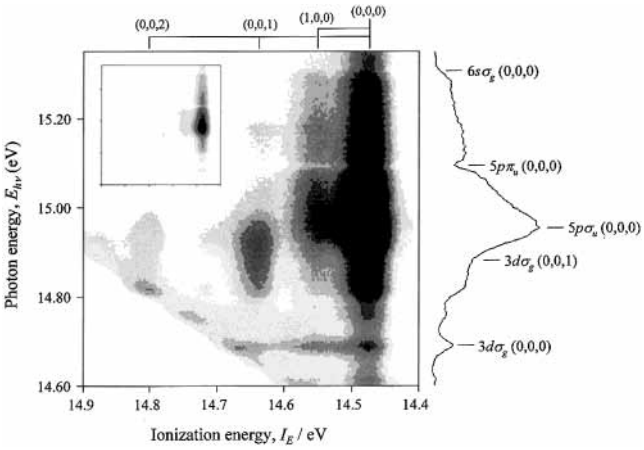

Figure 3. Two-dimensional photoelectron spectrum for the $CS_2^+(\tilde{B}\ ^2\Sigma_u^+)$ band and its vicinities measured in the photon energy range of 14.60−15.35 eV. See the caption of Figure 1.

normal incidence monochromator equipped with a concave 1200 lines/mm grating. The monochromatized photon beam is introduced into an ionization chamber that has a housing of 18 mm length and 28 mm diameter. The photon beam focused in the ionization chamber is about 0.5 × 3 mm^2 in size, and is estimated to be about 85% linearly polarized. The photon intensity is monitored by a photomultiplier with a sodium salicylate-coated window. Commercial CS_2 sample with 99% purity was subjected to repeated freeze−thaw−degassing cycles under vacuum and was then admitted into the ionization chamber. The effective pressure inside the chamber was estimated to be 3 × 10^{-4} Torr.

The electrons emitted on photoionization are detected by a 160° spherical electrostatic electron energy analyzer with the mean radius of the electron orbit of 54.7 mm (Comstock, AC-902). The analyzer is placed in the perpendicular direction to the electric vector of the photon beam, and equipped with a position-sensitive detector composed of dual microchannel plate multipliers and a two-dimensional resistive anode encoder (Quantar Technology, 3390A). The electron transmission efficiency as a function of electron kinetic energy was corrected using the $Ar^+(^2P_{3/2,1/2})$ band and a reported differential partial photoionization cross section.[20,21] Two-dimensional photoelectron spectra are measured by taking photoelectron spectra consecutively at wavelength intervals of 0.3 Å. A photon energy bandwidth of ∼ 0.8 Å (15 meV at 15 eV) and an analyzer resolution of ∼40 meV were maintained in the course of two-dimensional photoelectron spectroscopy.

Results

A. Two-Dimensional Photoelectron Spectra. Figures 1−3 show two-dimensional photoelectron spectra (2D-PESs) of CS_2 measured in the photon energy $E_{h\nu}$ region of 14.60−15.35 eV. The three spectra cover the ionization energies I_E for the $\tilde{X}\ ^2\Pi_g$, $\tilde{A}\ ^2\Pi_u$, and $\tilde{B}\ ^2\Sigma_u^+$states of CS_2^+.[22] In each spectrum the vertical axis corresponds to $E_{h\nu}$, and horizontal to I_E which is derived from the electron kinetic energy E_k by using the relation of $I_E = E_{h\nu} - E_k$. The photoelectron yield is presented as contour plots with eight tones from light to dark on a linear scale. The intense structures are truncated for the purpose of clarifying the weaker ones. The insets of Figures 1 and 3 show spectra whose scales are, respectively, twice and five times as high as those of the main panels. Below $E_k = E_{h\nu} - I_E$ = 0.5 eV in Figure 3, the accuracy of the electron yields is relatively low because of a rapid increase in both secondary electrons and transmission efficiency of the analyzer.

The right panels of the 2D-PESs show the curves obtained by plotting electron counts summed over the whole I_E range as a function of $E_{h\nu}$: these curves correspond to the constant-ionic-state (CIS) spectra for the ionic bands. The curves are in good agreements with the CIS spectra reported by Locht et al.[15] and exhibit five resonances at $E_{h\nu}$ = 14.69, 14.88, 14.95, 15.09, and 15.31 eV. The energy levels are indicated in Figures 1−3. Three resonances at $E_{h\nu}$ = 14.95, 15.09, and 15.31 eV, the latter two of which are window types, have been categorized into the vibrational ground Rydberg states $CS_2^*(R_C)$ converging to $CS_2^+(\tilde{C}\ ^2\Sigma_g^+)$.[19,23] Their effective quantum numbers n^* are calculated using I_E = 16.1883 eV[22] of $CS_2^+(\tilde{C}\ ^2\Sigma_g^+)$ to be 3.32, 3.52, and 3.94, and they are assigned to the $5p\sigma_u$, $5p\pi_u$, and $6s\sigma_g$ states, respectively. Excitation to the $6s\sigma_g$ state results from an electric quadrupole transition. The resonance at $E_{h\nu}$ = 14.69 eV has been assigned by Wu and Judge to the $4p\sigma_u$- or $3d\sigma_g$-type Rydberg state $CS_2^*(R_D)$ converging to $CS_2^+(\tilde{D}\ ^2\Pi_u)$,[10]

TABLE 1: Preferences in Autoionization of Resonance States Which Are Judged from the CIS Spectra in Figures 1−3. Vibrational Branching Ratios Are Given for the Autoionization of $3d\sigma_g$ (0,0,1) into $CS_2^+(\tilde{X}\ ^2\Pi_g$ and $\tilde{B}\ ^2\Sigma_u^+)$. These Ratios Are Derived from the One-Dimensional Photoelectron Spectra in Figures 5 and 6

		ionic states produced by autoionization		
$E_{h\nu}$ (eV)	assignments	$CS_2^+(\tilde{X}\ ^2\Pi_g)$	$CS_2^+(\tilde{A}\ ^2\Pi_u)$	$CS_2^+(\tilde{B}\ ^2\Sigma_u^+)$
14.69	$3d\sigma_g$ (0,0,0) [a]	medium	weak	strong
14.88	$3d\sigma_g$ (0,0,1) [a]	medium [(0,0,0)/(0,0,1) = 0.18] [c]	weak	strong [(0,0,0)/(0,0,1) = 1.07] [c]
14.95	$5p\sigma_u$ (0,0,0) [b]	weak	weak	strong

[a] Present work. [b] References 19 and 23. [c] Vibrational branching ratio between the formation channels of the (0,0,0) and (0,0,1) levels.

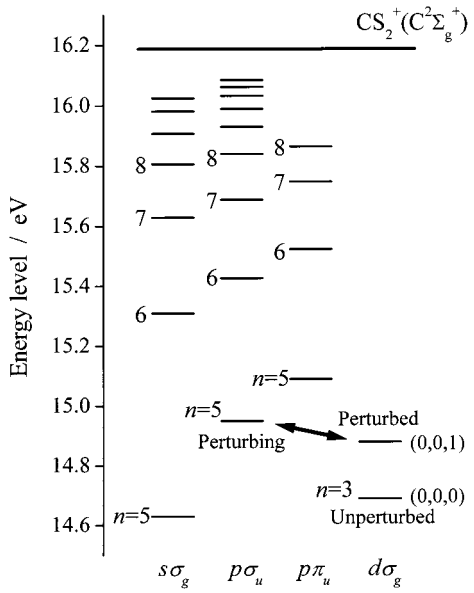

Figure 4. Energy-level diagram of the vibrational-ground Rydberg states converging to $CS_2^+(\tilde{C}\ ^2\Sigma_g^+)$ and the (0,0,1) level of the $3d\sigma_g$ state. All energies are measured with respect to the neutral ground state of $CS_2[\tilde{X}^1\Sigma_g^+$ (0,0,0)]. The energy levels for the $ns\sigma_g$, $np\sigma_u$, and $np\pi_u$ series are taken from refs 7 and 23. The arrow designates the vibronic interaction between the (0,0,0) level of $5p\sigma_u$ and the (0,0,1) level of $3d\sigma_g$.

where $CS_2^+(\tilde{D}\ ^2\Pi_u)$ is a satellite state associated with ionization of the $2\pi_u$ orbital.[22] We will propose an alternate assignment of the 14.69 eV resonance to the (0,0,0) level of the $3d\sigma_g$ $CS_2^*(R_C)$ state, as will be described in Discussion Section B. The resonance at $E_{h\nu} = 14.88$ eV which has been unclassified so far is the main concern of this paper. The energy-level diagram in Figure 4 summarizes the Rydberg states involved in the present study together with other high-lying states above 15.35 eV.

From the intensity of each resonance state in the CIS spectra we can derive preference in autoionization to the final ionic states. Such preferences are understood in terms of the nature of the orbitals involved in the autoionization process.[24,25] Among the five resonances, we focus our attention to the preferences of the resonances at $E_{h\nu} = 14.69$, 14.88, and 14.95 eV. The 14.69 eV resonance is observed moderately, weakly, and strongly in the CIS spectrum for the $\tilde{X}\ ^2\Pi_g$, $\tilde{A}\ ^2\Pi_u$, and $\tilde{B}\ ^2\Sigma_u^+$ states of CS_2^+, respectively. The 14.88 eV resonance appears to follow a similar trend, but its preference somewhat depends on the final vibrational level as mentioned later. In contrast, the $5p\sigma_u$ $CS_2^*(R_C)$ state at $E_{h\nu} = 14.95$ eV is hardly observed in the CIS spectra for $CS_2^+(\tilde{X}\ ^2\Pi_g$ and $\tilde{A}\ ^2\Pi_u)$. These preferences are summarized in Table 1.

It is probable that the vibrational features of CS_2^+ produced by direct ionization in Figures 1−3 are essentially the same as those obtained by using He I photoelectron spectroscopy, since contribution from autoionization of any superexcited states can be dismissed at $E_{h\nu} = 21.22$ eV. From this viewpoint, we can assume that the following vibrational features in a reported high-resolution He I photoelectron spectrum[22] of CS_2 prevail throughout the entire region of our 2D-PESs: The $CS_2^+(\tilde{X}\ ^2\Pi_g)$ band is dominated by the (0,0,0) level splitting into the spin−orbit components, the $CS_2^+(\tilde{A}\ ^2\Pi_u)$ band consists of a ν_1 vibrational progression with the spin−orbit splitting of ∼22 meV, and, in the $CS_2^+(\tilde{B}\ ^2\Sigma_u^+)$ band, the (0,0,0) level is about nine times as intense as the second strongest (1,0,0) level.

At the resonant $E_{h\nu}$ positions, the 2D-PESs must be affected by autoionization of superexcited states in addition to direct ionization. Figures 1−3, however, reveal that vibrational distributions of CS_2^+ at the vibrational ground $5p\sigma_u$, $5p\pi_u$, and $6s\sigma_g$ $CS_2^*(R_C)$ states behave similarly to those due to direct ionization, though the whole intensities of the band are modulated. This similar behavior can be accounted for by the following argument. The relative intensity of the (0,0,0) level of $CS_2^+(\tilde{C}\ ^2\Sigma_g^+)$ is ∼10 times as high as that of the second strongest (1,0,0) level in a He I photoelectron spectrum,[22] which suggests that $CS_2^+(\tilde{C}\ ^2\Sigma_g^+)$ and $CS_2(\tilde{X}\ ^1\Sigma_g^+)$ have potential energy surfaces of similar shape around the equilibrium geometry. Since the potential energy surface of $CS_2^*(R_C)$ is considered to be quite similar to that of $CS_2^+(\tilde{C}\ ^2\Sigma_g^+)$ on the basis of the core ion model,[26] the potential energy surface around the equilibrium geometry of each $CS_2^*(R_C)$ state also resembles that of $CS_2(\tilde{X}\ ^1\Sigma_g^+)$. Ionic vibrational distribution due to autoionization is determined by the Franck−Condon factors between the superexcited and ionic states. As a consequence, autoionization of the vibrational ground $CS_2^*(R_C)$ and direct photoionization of the vibrational ground $CS_2(\tilde{X}\ ^1\Sigma_g^+)$ lead to similar vibrational distributions of CS_2^+.

B. Autoionizing Features at $E_{h\nu} = 14.88$ eV. Characteristic vibrational structures at $E_{h\nu} \sim 14.88$ eV emerge on the 2D-PESs for the $CS_2^+(\tilde{X}\ ^2\Pi_g$ and $\tilde{B}\ ^2\Sigma_u^+)$ bands in Figures 1 and 3. Emergence at the specific $E_{h\nu}$ positions means that the vibrational structures originate not from direct ionization but from autoionization of a superexcited state. As to the 2D-PES for $CS_2^+(\tilde{A}\ ^2\Pi_u)$, we cannot recognize any anomaly in the vibrational feature around $E_{h\nu} = 14.88$ eV, corresponding to the unfavorable autoionization of the superexcited state into the $CS_2^+(\tilde{A}\ ^2\Pi_u)$ state (see Table 1). To extract the characteristic vibrational structures more clearly from Figures 1 and 3, one-dimensional photoelectron spectra are obtained by summing electron counts at every I_E over the $E_{h\nu} = 14.80-14.95$ eV range along the $E_{h\nu}$ direction. The resultant spectra are illustrated in Figures 5 and 6, respectively, where the intensity is represented in the same scale.

In Figure 5, there exist two peaks at $I_E = 10.23$ and 10.28 eV, corresponding to the intense spots in Figure 1, in addition to the spin−orbit components of the vibrational ground state of $CS_2^+(\tilde{X}\ ^2\Pi_g)$. The peaks can be assigned to the spin−orbit components of the (0,0,1) level, whose I_E values agree well with those reported, 10.2251 and 10.2812 eV.[22] The one-dimensional

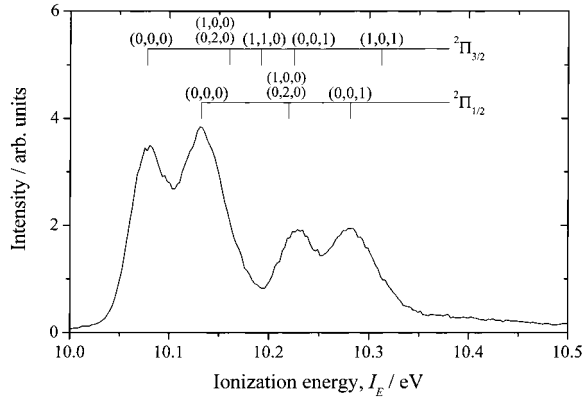

Figure 5. One-dimensional photoelectron spectrum for the $CS_2^+(\tilde{X}\ ^2\Pi_g)$ band, which is obtained by summing electron counts in Figure 1 at every I_E over the $E_{h\nu} = 14.80-14.95$ eV range along the $E_{h\nu}$ direction. Vibrational levels are indicated at the I_E positions reported in ref 22.

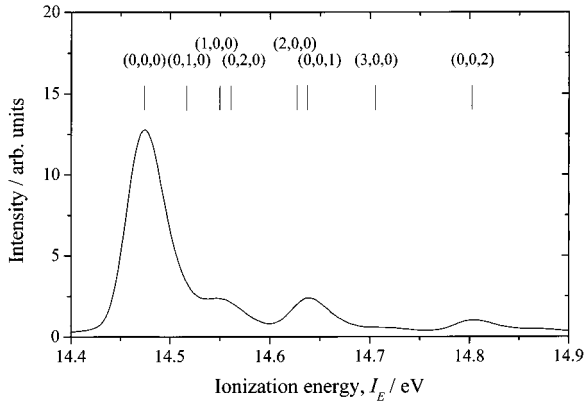

Figure 6. One-dimensional photoelectron spectrum for the $CS_2^+(\tilde{B}\ ^2\Sigma_u^+)$ band, which is obtained by summing electron counts in Figure 3 at every I_E over the $E_{h\nu} = 14.80-14.95$ eV range along the $E_{h\nu}$ direction. Vibrational levels are indicated at the I_E positions reported in ref 22.

photoelectron spectrum of $CS_2^+(\tilde{B}\ ^2\Sigma_u^+)$ in Figure 6 also manifests the formation of the $v_3 = 1$ and 2 vibrational states. It should be noted that the relative electron yield of the $v_3 = 2$ peak is not reliable because there is a large uncertainty in the transmission efficiency of the analyzer at $E_k < 0.5$ eV. The assignments are based on the reported I_E values: i.e., 14.6371 and 14.8020 eV for the (0,0,1) and (0,0,2) levels, respectively.[22] The reported He I photoelectron spectra show the formation of the (0,0,1) levels of $CS_2^+(\tilde{X}\ ^2\Pi_g)$ and $CS_2^+(\tilde{B}\ ^2\Sigma_u^+)$ promoted through the vibronic interaction with $CS_2^+(\tilde{A}\ ^2\Pi_u)$ and $CS_2^+(\tilde{C}\ ^2\Sigma_g^+)$, respectively.[22] Nevertheless, the relative intensity of the (0,0,1) level is much higher in Figures 1 and 3 than in the He I photoelectron spectra.

By a comparison between the one-dimensional photoelectron spectrum in Figure 5 and that measured at $E_{h\nu} < 14.80$ eV, we allocate most of the (0,0,1) counts and approximately 10% of the (0,0,0) counts in Figure 5 to autoionization of the resonance state. In the same way, essentially all of the (0,0,1) counts and approximately 20% of the (0,0,0) counts in Figure 6 are allocated to the autoionization. Here, the contribution from the autoionization of $5p\sigma_u$ $CS_2^*(R_C)$ is properly subtracted by comparing Figure 6 with one-dimensional photoelectron spectra measured at $E_{h\nu} > 14.95$ eV, because this contribution is not negligible as can be judged from the CIS spectrum for $CS_2^+(\tilde{B}\ ^2\Sigma_u^+)$ in Figure 3. The vibrational branching ratios of the (0,0,0) to (0,0,1) levels are calculated from the allocated signal counts to be 0.18 and 1.07 for the autoionization into $CS_2^+(\tilde{X}\ ^2\Pi_g)$ and $CS_2^+(\tilde{B}\ ^2\Sigma_u^+)$, respectively. These values are subjoined in Table 1. The vibrational distributions are strikingly different for different final ionic states. These different distributions are related to the dependence of the preference in autoionization on the final vibrational levels of CS_2^+. The details will be described in Discussion Section C.

Discussion

A. Formation Mechanism of the CS_2^+ States Excited in the ν_3 Mode. Vibrational distributions of $CS_2^+(\tilde{X}\ ^2\Pi_g$ and $\tilde{B}\ ^2\Sigma_u^+)$ at $E_{h\nu} = 14.88$ eV are determined by the Franck−Condon factor between the superexcited and CS_2^+ states. On the normal coordinate for the ν_3 mode, overlap vanishes between the symmetric vibrational wave functions for the even-v_3 levels of the superexcited state and antisymmetric wave functions for $v_3^+ = 1$ of the CS_2^+ states. Here, v_3^+ denotes the vibrational quantum of the ν_3 mode of CS_2^+. Consequently, we must consider the odd-v_3 vibrational levels of the superexcited-state alone to interpret a preferential formation of the ionic (0,0,1) levels.

Within the approximation rooted in the Franck−Condon principle no odd-v_3 level can be produced by the electric dipole transition from the vibrational ground state of $CS_2(\tilde{X}\ ^1\Sigma_g^+)$. The transition to an odd v_3 level becomes allowed by vibronic interaction occurring in a symmetry forbidden superexcited state. If the resonance at $E_{h\nu} = 14.88$ eV results from transition to $v_3 \geq 3$ vibrational state, other characteristic structures due to the transition to the $v_3 = 1$ state would appear at a lower $E_{h\nu}$ position on 2D-PESs in Figures 1 and 3. A closer inspection on the 2D-PESs reveals no discernible enhancement of the $v_3^+ = 1$ level anywhere except at $E_{h\nu} = 14.88$ eV. We therefore attribute the resonance at $E_{h\nu} = 14.88$ eV to the (0,0,1) level of a symmetry-forbidden superexcited state.

An alternate mechanism for the formation of such an odd-v_3 level of a superexcited state is a conversion from an even-v_3 level of a dipole-allowed superexcited state initially formed to an odd-v_3 level of another neutral state. This mechanism is, however, much less plausible, since the conversion is inefficient due to the vanishing overlap between the vibrational wave functions. In the following section, we devote ourselves to give a definite assignment of the 14.88 eV state on the assumption that the formation of the odd-v_3 level is promoted by vibronic interaction. This assumption will be shown to be self-consistent in the assignment procedure and compatible with all of the resonance features in the CIS spectra of Figures 1−3. In contrast, there is no direct evidence in favor of the above two-step autoionization.

B. Assignment of the Forbidden Superexcited State. The transition to the (0,0,1) level of the symmetry-forbidden state at $E_{h\nu} = 14.88$ eV is considered to borrow the intensity from that to a neighboring allowed electronic state with symmetry of Σ_u^+ or Π_u. Here, proximity between the two states is critically important. The intense (0,0,0) level of the $5p\sigma_u$ $CS_2^*(R_C)$ state is lying just above the (0,0,1) level of the symmetry-forbidden state. The $5p\sigma_u$ $CS_2^*(R_C)$ state with the $(6\sigma_g)^{-1}(5p\sigma_u)^1\ ^1\Sigma_u^+$ configuration is therefore most likely to be the main intensity-lending state to the forbidden state. This assumption is strongly supported by additional evidence: the peak shape of the $5p\sigma_u$ resonance is broad (∼150 meV fwhm) and the quantum defect is smaller than the higher members belonging to the same Rydberg series.[6,8,14] This evidence indicates an interaction of the $5p\sigma_u$ state with the lower forbidden state at $E_{h\nu} = 14.88$ eV. In general the intensity borrowing occurs between vibronic levels with the same symmetry, so that the overall symmetry for the (0,0,1) level of

the forbidden state should agree with that for the intensity-lending state, i.e., Σ_u^+. Since the symmetry of the (0,0,1) vibration is σ_u^+, the electronic part of the symmetry-forbidden superexcited state turns out to have the Σ_g^+ symmetry.

Possible candidates for this Σ_g^+-type forbidden superexcited state are several $CS_2^*(R_C)$ and $CS_2^*(R_D)$ states with a low principal quantum number n. The $CS_2^*(R_C)$ states have the same ion core as the intensity-lending $5p\sigma_u$ $CS_2^*(R_C)$. On the contrary, the ion core of $CS_2^*(R_D)$ is different with four occupied orbitals from that of $5p\sigma_u$ $CS_2^*(R_C)$. Moreover, we can anticipate that $CS_2^*(R_D)$ state shows a broad and diffuse feature, judging from the diffuse $CS_2^+(\tilde{D}\ ^2\Pi_u)$ band (~400 meV fwhm) even in a high-resolution He I photoelectron spectrum.[22] For these reasons, the $CS_2^*(R_D)$ states are much less plausible for the forbidden state at $E_{h\nu} = 14.88$ eV.

Provided that the forbidden state belongs to one of the $CS_2^*(R_C)$ series, its effective quantum number is calculated from $I_E = 16.3967$ eV for the (0,0,1) level of $CS_2^+(\tilde{C}\ ^1\Sigma_g^+)$[22] to be $n^* = 3.00$. From this n^* value the $3d\sigma_g$ and $5s\sigma_g$ members are reasonable. Wilden and Comer have determined the excitation energy for the vibrational ground state of $5s\sigma_g$ to be 14.63 eV.[23] The (0,0,0) level of the forbidden state is however expected to lie at $E_{h\nu}$ which is a little higher than 14.67 eV, because the (0,0,0)−(0,0,1) separation of this state may be smaller than that of $CS_2^+(\tilde{C}\ ^2\Sigma_g^+)$, 0.2084 eV,[22] owing to the interaction between the (0,0,1) level at $E_{h\nu} = 14.88$ eV and the (0,0,0) level of $5p\sigma_u$ $CS_2^*(R_C)$ at $E_{h\nu} = 14.95$ eV. The $5s\sigma_g$ $CS_2^*(R_C)$ state is thereby ruled out, and consequently we assign the forbidden superexcited state to $3d\sigma_g$ $CS_2^*(R_C)$. In summary, the (0,0,1) level of the $3d\sigma_g$ state is perturbed with the (0,0,0) level of the $5p\sigma_u$ state through the vibronic interaction, and the transition to the former level borrows the intensity from that to the latter level (see Figure 4).

Next, we will concern ourselves with the peaks at $E_{h\nu} = 14.69$ eV in Figures 1 and 3. In this connection, reported electron energy loss spectra[23] showed an enhancement at 14.69 eV at low incident electron energies, suggesting a forbidden electronic transition. We conceive that the 14.69 eV features in our 2D-PESs and previous electron energy loss spectra stem from the same superexcited state, that is, the vibrational ground $3d\sigma_g$ $CS_2^*(R_C)$ state to which excitation becomes allowed through an electric quadrupole transition. Indeed, the 14.69 eV features are located in such a position as to match with the excitation energy expected from the (0,0,0)−(0,0,1) separation mentioned in the preceding paragraph. Moreover, the present assignment is supported by the preference in the autoionization: the 14.69 and 14.88 eV resonances show a similar preference (see Table 1).

One may suppose that the (0,0,1) level of the $nd\sigma_g$ $CS_2^*(R_C)$ state with $n \geq 4$ would also be allowed through an interaction with the $(n + 2)p\sigma_u$ $CS_2^*(R_C)$ state. Nevertheless, there is no noticeable spot of the (0,0,1) level of $CS_2^+(\tilde{X}\ ^2\Pi_g$ or $\tilde{B}\ ^2\Sigma_u^+)$ on two-dimensional photoelectron spectra in a wider $E_{h\nu}$ region. We can consider three reasons for the absence. First, the interaction strength decreases with the increase of n, because the overlap between wave functions of the interacting Rydberg states becomes less favorable with increasing n. Second, photoexcitation strength from the ground state decreases with increasing n, since it is roughly proportional to the orbital extent of the Rydberg electron. Third, the proximity between the (0,0,1) level of the $nd\sigma_g$ state and the vibrational ground $(n + 2)p\sigma_u$ state gets worse, since the term value becomes closer between the vibrational ground states of $nd\sigma_g$ and $(n + 2)p\sigma_u$ but the separation between the (0,0,0) and (0,0,1) levels of $nd\sigma_g$ $CS_2^*(R_C)$ is essentially the same.

C. Vibronic Interaction Affecting Distinctive Preferences in Autoionization. Overlap is zero between the vibrational wave functions of the (0,0,1) level of $3d\sigma_g$ $CS_2^*(R_C)$ at $E_{h\nu} = 14.88$ eV and the (0,0,0) level of CS_2^+. Nevertheless, the autoionization of the (0,0,1) level of $3d\sigma_g$ $CS_2^*(R_C)$ allows the (0,0,0) levels of $CS_2^+(\tilde{X}\ ^2\Pi_g$ and $\tilde{B}\ ^2\Sigma_u^+)$ to be produced, as described in the last paragraph of Results Section B. This implies that the coupling between electron motion and molecular vibration has an effect not only on the primary photoexcitation but on subsequent autoionization processes. That is, there still remains the mixing of the (0,0,1) level of $3d\sigma_g$ $CS_2^*(R_C)$ at $E_{h\nu} = 14.88$ eV with the (0,0,0) level of $5p\sigma_u$ $CS_2^*(R_C)$ at $E_{h\nu} = 14.95$ eV. Hence, the autoionization into the (0,0,0) level of CS_2^+ is considered to proceed through electron exchange mechanism involving the perturbing $5p\sigma_u$ $CS_2^*(R_C)$ state and the CS_2^+ continuum state, whereas that into the (0,0,1) level through the mechanism involving the zeroth-order $3d\sigma_g$ $CS_2^*(R_C)$ state and the CS_2^+ continuum state.

On the basis of the above discussion we can make two plausible predictions about the preference in the autoionization of the (0,0,1) level of $3d\sigma_g$ $CS_2^*(R_C)$ at $E_{h\nu} = 14.88$ eV. In what follows, this level will be referred to as the perturbed level, the (0,0,0) level of $5p\sigma_u$ $CS_2^*(R_C)$ at $E_{h\nu} = 14.95$ eV as the perturbing level, and the (0,0,0) level of $3d\sigma_g$ $CS_2^*(R_C)$ at $E_{h\nu} = 14.69$ eV as the unperturbed level. First, the perturbed and perturbing levels are expected to show a similar manner of electronic branching upon the autoionization into the (0,0,0) level of CS_2^+. Second, the perturbed and unperturbed levels show a similar form of electronic branching upon autoionization into the (0,0,1) level of CS_2^+. As evidenced from the autoionization preferences and vibrational branching ratios in Table 1, the perturbed level autoionizes much more preferentially into the (0,0,0) level of $CS_2^+(\tilde{B}^2\ \Sigma_u^+)$ than into that of $CS_2(\tilde{X}\ ^2\Pi_g)$. A similar trend is found in the autoionization preference of the perturbing level. On the other hand, the strong preference for $CS_2^+(\tilde{B}\ ^2\Sigma_u^+)$ is suppressed when the perturbed level autoionizes into the (0,0,1) levels, as indicated from the small (0,0,0)/(0,0,1) ratio for $CS_2^+(\tilde{X}\ ^2\Pi_g)$. Indeed, this preference of the perturbed level appears to resemble that of the unperturbed level.

Conclusion

We have measured 2D-PESs of CS_2 in the $E_{h\nu}$ region of 14.60−15.35 eV, to investigate excitation and decay mechanisms of superexcited states. The 2D-PESs show pronounced formation of the (0,0,1) levels of $CS_2^+(\tilde{X}\ ^2\Pi_g$ and $\tilde{B}\ ^2\Sigma_u^+)$ from a superexcited state at $E_{h\nu} = 14.88$ eV. This unusual vibrational excitation of ions in the ν_3 mode results from autoionization of the (0,0,1) level of the dipole-forbidden state which has been assigned to the $3d\sigma_g$ $CS_2^*(R_C)$ state conversing to $CS_2^+(\tilde{C}\ ^2\Sigma_g^+)$. The primary photoexcitation to the (0,0,1) level of the $3d\sigma_g$ state is considered to become allowed by vibronic interaction with the $5p\sigma_u$ $CS_2^*(R_C)$ state. We have additionally uncovered that the preference in autoionization of the $3d\sigma_g$ state into the final ionic states depends on their vibrational levels. The preference concerning the ionic (0,0,0) levels is explained in terms of the vibronic interaction that remains until autoionization, while the vibronic interaction is relatively uninfluential on the autoionization into the ionic (0,0,1) levels.

Acknowledgment. We gratefully acknowledge continuous support and valuable discussion from Dr. Hideo Hattori. Our thanks are also due to the members of the UVSOR for their

help during the course of the experiments. This work has been supported financially in part by national funds appropriated for special research projects of the Institute for Molecular Science, by a Grant-in-Aid for Scientific Research (Grant No. 10640504) from the Ministry of Education, Science, Sports, and Culture, Japan, and by a grant for scientific research from Matsuo Foundation.

References and Notes

(1) Sokell, E.; Wills, A. A.; Ćubric, D.; Currell, F. J.; Comer, J.; Hammond, P. *J. Electron Spectrosc. Relat. Phenom*. **1998**, *94*, 107, and references therein.

(2) Mitsuke, K.; Hikosaka, Y.; Hikida, T.; Hattori, H. *J. Electron Spectrosc. Relat. Phenom.* **1996**, *79*, 395.

(3) Mitsuke, K.; Hattori, H.; Hikosaka, Y. *J. Electron Spectrosc. Relat. Phenom.* **2000**, *112*, 137.

(4) Hattori, H.; Mitsuke, K. *J. Electron Spectrosc. Relat. Phenom.* **1996**, *80*, 1.

(5) Hattori, H.; Hikosaka, Y.; Hikida, T.; Mitsuke, K. *J. Chem. Phys.* **1997**, *106*, 4902.

(6) Tanaka, Y.; Jursa, A. S.; LeBlanc, F. J. *J. Chem. Phys.* **1960**, *32*, 1205.

(7) Cook, G. R.; Ogawa, M. *J. Chem. Phys.* **1969**, *51*, 2419.

(8) Ogawa, M.; Chang, H. C. *Can. J. Phys.* **1970**, *48*, 2455.

(9) Ono, Y.; Linn, S. H.; Prest, H. F.; Gress, M. E.; Ng, C. Y. *J. Chem. Phys.* **1980**, *73*, 2523.

(10) Wu, C. Y. R.; Judge, D. L. *J. Chem. Phys.* **1983**, *78*, 2180.

(11) Dibeler, V. H.; Walker, J. A. *J. Opt. Soc. Am.* **1967**, *57*, 1007.

(12) Brehm, B.; Eland, J. H. D.; Frey, R.; Kustler, A. *Int. J. Mass Spectrom. Ion Phys.* **1973**, *12*, 213.

(13) Eland, J. H. D.; Berkowitz, J. *J. Chem. Phys.* **1979**, *70*, 5151.

(14) Coppens, P.; Reynaert, J. C.; Drowart, J. *J. Chem. Soc., Faraday Trans. 2* **1979**, *75*, 292.

(15) Locht, R.; Hottmann, K.; Denzer W.; Baumgärtel, H. *BESSY Jahresber* **1993**, 148.

(16) Wu, C. Y. R.; Yih, T. S.; Judge, D. L. *Int. J. Mass Spectrom. Ion Phys.* **1986**, *68*, 303.

(17) Poliakoff, E. D.; Dehmer, J. L.; Parr, A. C.; Leroi, G. E. *J. Chem. Phys.* **1987**, *86*, 2557.

(18) Karawajczyk, A.; Erman, P.; Rachlew, E.; Stankiewicz, M.; Franzén, K. Y. *Chem. Phys. Lett.* **1998**, *285*, 373.

(19) Larzilliere, M.; Damany, N. *Can. J. Phys.* **1978**, *56*, 1150.

(20) Marr, G. V.; West, J. B. *Atomic Data Nucl. Data Tables* **1976**, *18*, 497.

(21) Holland, D. M. P.; Parr, A. C.; Ederer, D. L.; Dehmer J. L.; West, J. B. *Nucl. Instrum. Methods Phys. Res.* **1982**, *195*, 331.

(22) Baltzer, P.; Wannberg, B.; Lundqvist, M.; Karlsson, L.; Holland, D. M. P.; MacDonald, M. A.; Hayes, M. A.; Tomasello, P.; von Niessen, W. *Chem. Phys.* **1996**, *202*, 185.

(23) Wilden, D. G.; Comer, *J. Chem. Phys.* **1980**, *53*, 77.

(24) Eland, J. H. D. *Mol. Phys.* **1980**, *40*, 917.

(25) Mitsuke, K.; Hattori, H.; Yoshida, H. *J. Chem. Phys.* **1993**, *99*, 6642.

(26) Freund, R. S. In *Rydberg States of Atoms and Molecules*; edited by Stebbings, R. F., Dunning, F. B., Eds.; Cambridge University Press: Cambridge, 1983; Chapter 10.